Theoretical investigation of the double-β processes in ^{96}Ru

Jouni Suhonen
Department of Physics, P.O. Box 35 (YFL), FI-40014 University of Jyväskylä, Finland
(Received 26 March 2012; revised manuscript received 17 July 2012; published 3 August 2012)

The two-neutrino ($2\nu2\beta$) and neutrinoless ($0\nu2\beta$) double-β decays of ^{96}Ru are investigated for the transitions to the ground state, 0^+_{gs}, and 0^+ and 2^+ excited states in ^{96}Mo by using the quasiparticle random-phase approximation combined with the multiple-commutator model. G-matrix-based nuclear forces are used in realistic single-particle model spaces. All the possible channels, $\beta^+\beta^+$, β^+EC, and ECEC, are discussed for both the $2\nu2\beta$ and $0\nu2\beta$ decays. The associated half-lives are computed, in particular the one corresponding to the resonant neutrinoless double electron capture (R0νECEC) transition to the 2.712.68-MeV nuclear state in ^{96}Mo. This work represents the most complete theoretical investigation of the double-β-decay properties of ^{96}Ru thus far.

DOI: 10.1103/PhysRevC.86.024301 PACS number(s): 21.60.Jz, 23.40.Bw, 23.40.Hc, 27.60.+j

I. INTRODUCTION

Modern neutrino-oscillation experiments have brought the study of neutrino properties to the era of precision measurements. At the same time the fundamental character (Majorana or Dirac) of the neutrino is still unknown, as is also its absolute mass scale. To gain information on these two unknowns, atomic nuclei can be engaged as the mediators of Majorana-neutrino triggered neutrinoless double-β ($0\nu2\beta$) decays. The key issue here is how to cope with the involved nuclear-structure issues of the decays, crystallized in the form of the nuclear matrix elements (NMEs) [1–3]. To be able to exploit the potential data extracted from the $0\nu2\beta$-decay experiments one needs to evaluate the NMEs in a reliable enough way. It has become customary to employ the neutrino-emitting correspondent of $0\nu2\beta$ decay, the two-neutrino double-β ($2\nu2\beta$) decay, to confine the nuclear-model degrees of freedom in the NME calculations. The $2\nu2\beta$ decay is a second-order process in the standard model of the electroweak interactions and the associated half-lives have been measured for several nuclei [4].

Double-β^- decays have been studied intensively over the years [2,3] due to their favorable decay Q values. The positron-emitting modes of decays, $\beta^+\beta^+$, β^+EC, and ECEC are much less studied. The general, nuclear-model-independent frameworks of theory for these decays have been investigated in Ref. [5] for the $2\nu2\beta$-decay channels $\beta^+\beta^+$, β^+EC, and ECEC and in Ref. [6] for the $0\nu2\beta$-decay channels $\beta^+\beta^+$ and β^+EC. The formalism for the resonant neutrinoless double electron capture (R0νECEC) was first developed in Ref. [7] and later discussed and extended to its radiative variant ($0\nu\gamma$ECEC) in Ref. [8]. At present the resonant mode of 0νECEC decays is considered to have great potential for discovery of the Majorana mass of the neutrino. That is why much experimental effort is being invested in observing this mode of decay.

The various $2\nu2\beta$ and $0\nu2\beta$ decay channels of ^{96}Ru were discussed in the early works of [9–11]. In all of these calculations only transitions to the final ground states were considered. Later the two-neutrino $\beta^+\beta^+$, β^+EC, and ECEC decays of ^{96}Ru were examined in Ref. [12] for both the ground states and first excited 0^+ states. In Ref. [13] a systematic study of the neutrinoless $\beta^+\beta^+$ and β^+EC decays to excited 0^+ states in, e.g., ^{96}Ru was performed. In these calculations the computational scheme was based on the relativistic harmonic confinement model (RHCM) of quarks and the resulting nucleon form factors [14–16]. In this framework a folding of the free nucleon current with the confined quark degrees of freedom was done, resulting in a nucleonic current that differed from that of the standard formulation [1,17]. In addition, no short-range correlations were taken into account beyond the RHCM-predicted nucleon form factors.

Nuclear-structure calculations associated with the R0νECEC processes were performed for ^{112}Sn in Refs. [7,18], for ^{74}Se in Ref. [19], for ^{136}Ce in Ref. [20], and for ^{106}Cd in Ref. [21]. General formalism of the associated nuclear-structure calculations were reviewed in Ref. [22]. No previous nuclear-structure calculations for the R0νECEC decay of ^{96}Ru have been done. It should be noted that also simple estimates of such NMEs have been used in the review presented in Ref. [23], where a global analysis of the possible resonant decays was performed.

In the present article the two-neutrino $\beta^+\beta^+$, β^+EC, and ECEC transitions and neutrinoless $\beta^+\beta^+$ and β^+EC transitions in ^{96}Ru are discussed. Considered are the transitions to the ground state, 0^+_{gs}, and to the first and second excited 0^+ states, 0^+_1 and 0^+_2, as well as to the first, second, and third 2^+ states, 2^+_1, 2^+_2, and 2^+_3. The $0\nu2\beta$ decays to only the 0^+ states are considered since large suppression of the mass mode for the $0\nu2\beta$ decays to 2^+ states is expected [24]. Furthermore, the R0νECEC transition to the possible resonant state at an excitation energy of 2718.41 keV is considered. Here the energy of the two electron L_1 holes in the molybdenum atom has been added to the state's nuclear excitation energy of 2712.68 keV.

In Ref. [23] it was analyzed that the resonant state at a nuclear excitation of 2712.68 keV γ decays to a state with spin-parity assignment 5^+ or 6^+. This would exclude the 0^+ assignment for the resonant state. In the present work, however, the analysis of the R0νECEC half-life is performed by assuming a 0^+ assignment for the resonant state. This assignment leads to a very likely enhancement in the decay rate and thus the calculated half-life should be taken as an optimistic estimate or a lower limit for the half-life. A similar situation is realized in the case of the R0νECEC decay of ^{106}Cd to the 2717.56-keV nuclear state in ^{106}Pd. In Ref. [21] this state

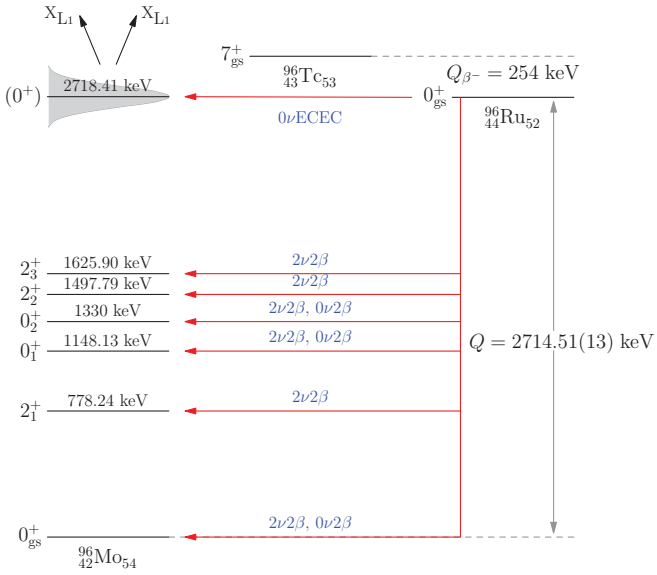

FIG. 1. (Color online) Experimental low-energy spectrum of ^{96}Mo and the resonant state at 2712.68 keV of excitation, assumed here to be a 0^+ state (for which the atomic two-L_1-hole energy has been added). The spin-parity of the resonant state is uncertain. All the double-β transition modes under consideration in this article are indicated by horizontal arrows. The Q value (difference of the atomic masses) has been taken from [35] and the level energies from [36].

was assigned to a 0^+ state while in fact a closer analysis [23] would point to a higher value of the angular momentum. In this case, as in the present one, the computed half-life could be considered as a rough estimate with optimistic inclination.

All the discussed decay transitions are displayed in Fig. 1. For all the $0\nu2\beta$ transitions the NMEs are computed by the use of both the Jastrow short-range correlations [25] and the unitary correlation operator method (UCOM) correlations [26,27]. Both short-range correlators have been recently used in many $0\nu\beta^-\beta^-$ calculations [28–33] and in some $0\nu\beta^+$/EC calculations [21]. In addition, the contributions arising from the induced currents and the finite nucleon size [34] have been taken into account. As is evident from above, the calculations of the present paper constitute the thus-far most complete and up-to-date treatment of the double-β-decay properties of ^{96}Ru.

In this work the wave functions of the nuclear states involved in double-β-decay transitions are calculated by the use of the quasiparticle random-phase approximation (QRPA) in a realistically large single-particle model space. (An exhaustive discussion on the model-space effects is given in Refs. [37–39].) In particular, the 2^+_1 and 2^+_3 states, as well as the resonant 0^+ state in ^{96}Ru, are assumed to be basic excitations (one-phonon states) of the charge-conserving QRPA (ccQRPA) [40], whereas the 0^+_2 state and 2^+_2 state are assumed to consist of two 2^+_1 ccQRPA phonons, as discussed in Refs. [38,39]. The J^π states of the intermediate nucleus ^{96}Tc of the $\beta\beta$ decays are generated by the usual proton-neutron QRPA (pnQRPA) [2,40]. The one- and two-phonon states in ^{96}Ru are then connected to the J^π states of ^{96}Tc by transition amplitudes obtained from a higher-QRPA framework called the multiple-commutator model (MCM), first introduced in Ref. [41] and further extended in Ref. [42].

II. OUTLINE OF THE THEORETICAL FRAMEWORK

In this section a rather detailed account of the basic theoretical ingredients of the calculations is given. In this way the reader can have a unified picture of the formalisms used for various types of double-β transitions.

A. Two-neutrino double-β decays

Two-neutrino double-β decay, $2\nu2\beta$, on the positron-emitting side can proceed through three different channels, namely, $\beta^+\beta^+$, β^+EC, and ECEC. The associated half-lives can be expressed as [1,5]

$$\left[T^\alpha_{2\nu}(I^+)\right]^{-1} = \frac{(Gg_{\rm A})^4 m_{\rm e}^9}{32\pi^7 \ln 2} \int dE^{(\alpha)} \mathcal{M}_\alpha(I^+), \quad \alpha = \beta^+\beta^+,\ \beta^+{\rm EC},\ {\rm ECEC}, \tag{1}$$

where $I = 0, 2$ is the final-state angular momentum, G is the weak-interaction constant, $g_{\rm A}$ is the axial-vector coupling constant, $m_{\rm e}$ is the electron rest mass, and $\int dE^{(\alpha)}$ denotes the integration over the lepton phase space. The integration is different for the three decay channels $\alpha = \beta^+\beta^+$, $\alpha = \beta^+$EC, and $\alpha =$ ECEC [5]. The combined nuclear and leptonic matrix element $\mathcal{M}_\alpha(I^+)$ can be written as [1,5]

$$\mathcal{M}_\alpha(0^+) = \frac{1}{4}\left|\sum_a M^\alpha_{{\rm GT}a}(0^+)\left(K^\alpha_a + L^\alpha_a\right)\right|^2 + \frac{1}{12}\left|\sum_a M^\alpha_{{\rm GT}a}(0^+)\left(K^\alpha_a - L^\alpha_a\right)\right|^2, \tag{2}$$

$$\mathcal{M}_\alpha(2^+) = \left|\sum_a M^\alpha_{{\rm GT}a}(2^+)\left(K^\alpha_a - L^\alpha_a\right)\right|^2, \tag{3}$$

for the decays to the $I^+ = 0^+, 2^+$ final states. Here the index a denotes the summation over the virtual states of the intermediate nucleus of the $2\nu2\beta$ decay and K^α_a and L^α_a are the energy denominators [1] that can be cast in the form

$$K^\alpha_a = \frac{1}{\Delta_a + E^\alpha_1} + \frac{1}{\Delta_a + E^\alpha_2}; \quad L^\alpha_a = K^\alpha_a(\nu_1 \leftrightarrow \nu_2), \tag{4}$$

where

$$\Delta_a = (E_a - M_i c^2)/m_{\rm e}c^2, \tag{5}$$

with E_a being the energy of the intermediate state a and M_i being the mass of the initial nucleus. The quantities E^α_1 and E^α_2 denote the total energies of the leptons active in the first and second decay vertex, respectively. The denominator L^α_a is obtained from K^α_a by the exchange of the emitted neutrinos.

We can separate the nuclear and leptonic degrees of freedom in Eqs. (2) and (3) by replacing in the denominators (4) the lepton energies E^α_1 and E^α_2 by their averages $\langle E^\alpha_1\rangle$ and $\langle E^\alpha_2\rangle$ obtained by assuming that the emitted leptons share democratically the decay energy W^α_0 of each decay mode.

It is also obvious that the latter term in the 0^+ matrix element (2) is negligible in comparison with the first term, because it has (a) a small prefactor, (b) a higher-order denominator in the nuclear matrix element, and (c) a suppressed lepton phase-space integral.

After the above-described maneuvers we end up with the following final expressions for the decay half-lives of the various modes:

$$\left[T_{2\nu}^{\beta^+\beta^+}(I^+)\right]^{-1} = G_{2\nu}^{\beta^+\beta^+}(I^+)\left[M_{2\nu}^{\beta^+\beta^+}(I^+)\right]^2, \tag{6}$$

$$\left[T_{2\nu}^{\beta^+\mathrm{EC}}(I^+)\right]^{-1} = G_{2\nu}^{\beta^+\mathrm{EC(K)}}(I^+)\left[M_{2\nu}^{\beta^+\mathrm{EC(K)}}(I^+)\right]^2 + G_{2\nu}^{\beta^+\mathrm{EC(L)}}(I^+)\left[M_{2\nu}^{\beta^+\mathrm{EC(L)}}(I^+)\right]^2, \tag{7}$$

$$\left[T_{2\nu}^{\mathrm{ECEC}}(I^+)\right]^{-1} = G_{2\nu}^{\mathrm{EC(K)EC(K)}}(I^+)\left[M_{2\nu}^{\mathrm{EC(K)EC(K)}}(I^+)\right]^2 + G_{2\nu}^{\mathrm{EC(K)EC(L)}}(I^+)\left[M_{2\nu}^{\mathrm{EC(K)EC(L)}}(I^+)\right]^2, \tag{8}$$

where the expressions for the lepton phase-space integrals $G_{2\nu}^{\alpha}(I^+)$, $\alpha = \beta^+\beta^+$, β^+EC, ECEC, are given in Ref. [5] and the NMEs $M_{2\nu}^{\alpha}(I^+)$ include the nuclear part of the denominators (4) and a summation over all the 1^+ states of the intermediate nucleus ^{96}Tc (see below). Above, the symbols EC(K) and EC(L) denote electron captures from the atomic K and L_1 shells, respectively.

The NMEs involved in the above half-life expressions can be cast in the form

$$M_{2\nu}^{\alpha}(I^+) = \sum_{k_1} M_{k_1}(I^+) F_{k_1}^{\alpha}(I^+); \quad \alpha = \beta^+\beta^+,\ \beta^+\mathrm{EC},\ \mathrm{ECEC}, \tag{9}$$

where in the QRPA framework one writes

$$M_{k_1}(I^+) = \frac{1}{\sqrt{1+2\delta_{I2}}} \sum_{k_2} \sum_{pp'nn'} m(nn', pp') \left(I_f^+ \| [c_{n'}^\dagger \tilde{c}_{p'}]_1 \| 1_{k_1}^+\right) \times \left\| 1_{k_1}^+ \middle| 1_{k_2}^+ \right\rangle \left(1_{k_2}^+ \| [c_n^\dagger \tilde{c}_p]_1 \| 0_i^+\right), \tag{10}$$

and the single-particle part is written as

$$m(nn', pp') = \tfrac{1}{3}(n' \| \boldsymbol{\sigma} \| p')(n \| \boldsymbol{\sigma} \| p), \tag{11}$$

the operator $\boldsymbol{\sigma}$ being the three components of the Pauli spin matrices. The label $p = n_p, l_p, j_p$ $(n = n_n, l_n, j_n)$ denotes the quantum numbers of the proton (neutron) single-particle states. The one-body transition densities $(I_f^+ \| [c_{n'}^\dagger \tilde{c}_{p'}]_1 \| 1_{k_1}^+)$ and $(1_{k_2}^+ \| [c_n^\dagger \tilde{c}_p]_1 \| 0_i^+)$, involved in Eq. (10), are given separately for the different types of I^+ final states f in Sec. II C. Furthermore, the overlap between the two sets of pnQRPA states used in the calculations is given by

$$\left\langle J_{k_1}^\pi \middle| J_{k_2}^\pi \right\rangle = \sum_{pn} \left[X_{pn}^{J_{k_2}^\pi} \bar{X}_{pn}^{J_{k_1}^\pi} - Y_{pn}^{J_{k_2}^\pi} \bar{Y}_{pn}^{J_{k_1}^\pi} \right] \tag{12}$$

and it takes care of the matching of the corresponding states in the two sets of states based on the initial and final even-even reference nuclei. The amplitudes X and Y ($\bar{X}$ and $\bar{Y}$) come from the pnQRPA calculation starting from the initial (final) nucleus of the double-β decay.

The quantities $F_{k_1}^{\alpha}(I^+)$ in Eq. (9) are the various denominators that derive from (4) upon the lepton averaging procedure and they assume the following forms:

$$F_k^{\beta^+\beta^+}(0^+) = \left(\Delta_k + \tfrac{1}{2}W_0\right)^{-1}, \tag{13}$$

$$F_k^{\beta^+\beta^+}(2^+) = \left(\Delta_k + \tfrac{1}{2}W_0\right)^{-3}, \tag{14}$$

$$F_k^{\beta^+\mathrm{EC}}(0^+) = \frac{1}{\Delta_k - \varepsilon_{\mathrm{b1}} + \frac{1}{3}W_0^{\beta^+\mathrm{EC}}} + \frac{1}{\Delta_k + \frac{2}{3}W_0^{\beta^+\mathrm{EC}}}, \tag{15}$$

$$F_k^{\beta^+\mathrm{EC}}(2^+) = \frac{\Delta_k + \frac{1}{2}W_0}{\left(\Delta_k - \varepsilon_{\mathrm{b1}} + \frac{1}{3}W_0^{\beta^+\mathrm{EC}}\right)^2 \left(\Delta_k + \frac{2}{3}W_0^{\beta^+\mathrm{EC}}\right)^2}, \tag{16}$$

$$F_k^{\mathrm{ECEC}}(0^+) = \frac{1}{\Delta_k - \varepsilon_{\mathrm{b1}} + \frac{1}{2}W_0^{\mathrm{ECEC}}} + \frac{1}{\Delta_k - \varepsilon_{\mathrm{b2}} + \frac{1}{2}W_0^{\mathrm{ECEC}}}, \tag{17}$$

$$F_k^{\mathrm{ECEC}}(2^+) = \frac{\Delta_k + \frac{1}{2}W_0}{\left(\Delta_k - \varepsilon_{\mathrm{b1}} + \frac{1}{2}W_0^{\mathrm{ECEC}}\right)^2 \left(\Delta_k - \varepsilon_{\mathrm{b2}} + \frac{1}{2}W_0^{\mathrm{ECEC}}\right)^2}, \tag{18}$$

where the normalized (by the electron rest-mass energy) intermediate energy is given by (5) and the decay energies are

$$W_0 = (M_i c^2 - E_f)/m_e c^2, \quad W_0^{\beta^+\mathrm{EC}} = W_0 + \varepsilon_{\mathrm{b1}}, \quad W_0^{\mathrm{ECEC}} = W_0 + \varepsilon_{\mathrm{b1}} + \varepsilon_{\mathrm{b2}}. \tag{19}$$

Here the quantity E_f is the final-state (ground-state or excited-state) energy and

$$\varepsilon_{\mathrm{b}i} = (m_e c^2 - B_i)/m_e c^2, \quad i = 1, 2, \tag{20}$$

where B_i is the binding energy of electron i in an atomic K or L_1 orbital [5]. In Δ_k [see Eq. (5)] E_k is the energy of the kth 1^+ state in ^{96}Tc. In the pnQRPA calculations the energy E_k is taken to be the average of the kth energy eigenvalues based on the two pnQRPA calculations, one for the initial and one for the final nucleus of the $\beta\beta$ decay. Furthermore, the energy difference $E_1 - M_i c^2$ is taken from experiment if the excitation energy of the first 1^+ state of the intermediate nucleus is known experimentally. At this point it is worth noting that in the present case the 1_1^+ energy in ^{96}Tc is not known experimentally, thus introducing an additional source of uncertainty. This problem is dealt with in Sec. IV.

B. Neutrinoless double-β decays

In this work it is assumed that the $0\nu2\beta$ decays proceed exclusively via the exchange of a massive Majorana neutrino. The inverse half-lives for the neutrinoless $\beta^+\beta^+$, β^+EC, and R0νECEC decays can be cast in the form

$$\left[T_{0\nu}^{\alpha}(0^+)\right]^{-1} = G_{0\nu}^{\alpha}(0^+) |M^{(0\nu)'}|^2 (|\langle m_\nu \rangle| [\mathrm{eV}])^2, \quad \alpha = \beta^+\beta^+,\ \beta^+\mathrm{EC}, \tag{21}$$

$$\left[T_{0\nu}^{\mathrm{ECEC}}(0^+)\right]^{-1} = G_{0\nu}^{\mathrm{ECEC}}(0^+) \left|M_{0\nu}^{\mathrm{ECEC}}\right|^2 \times \frac{|\langle m_\nu \rangle|^2 \Gamma}{(Q - E)^2 + \Gamma^2/4}, \tag{22}$$

where $\langle m_\nu \rangle$ is the effective neutrino mass [2] that should be given in Eq. (21) in units of electron volts. Furthermore, we define

$$M_{0\nu}^{\mathrm{ECEC}} = \frac{1}{R_A} M^{(0\nu)\prime}, \quad R_A = 1.2A^{1/3}\ \mathrm{fm}, \tag{23}$$

and the phase-space integrals $G_{0\nu}^{\beta^+\beta^+}(0^+)$ and $G_{0\nu}^{\beta^+\mathrm{EC}}(0^+)$ are defined in Ref. [6]. The phase-space integral for the R0νECEC mode can be written as

$$G_{0\nu}^{\mathrm{ECEC}}(0^+) = \left(\frac{G_{\mathrm{F}}\cos\theta_{\mathrm{C}}}{\sqrt{2}}\right)^4 \frac{g_{\mathrm{A}}^4}{4\pi^2 \ln 2} m_{\mathrm{e}}^6 \mathcal{N}_{0,-1}^2, \tag{24}$$

where $\mathcal{N}_{0,-1}$ is the normalization of the relativistic L_1-shell ($2\mathrm{s}_{1/2}$) Dirac wave function for a uniformly charged spherical nucleus [6]. For the presently discussed R0νECEC decay of ^{96}Ru the spin-parity assignment as 0^+ of the final state at 2712.68 keV of nuclear excitation is uncertain. For the decay width Γ the value $\Gamma = 0.082$ eV was adopted [43] and the Q value measurement of [35] gives for the degeneracy parameter $|Q - E| = 3.90$ keV.

The $0\nu 2b$ NMEs are defined in the standard way (see, e.g., [37–39]) in terms of the Gamow-Teller (GT), Fermi (F), and tensor (T) matrix elements

$$M^{(0\nu)\prime} = \left(\frac{g_{\mathrm{A}}}{1.25}\right)^2 \left[M_{\mathrm{GT}}^{(0\nu)} - \left(\frac{g_{\mathrm{V}}}{g_{\mathrm{A}}}\right)^2 M_{\mathrm{F}}^{(0\nu)} + M_{\mathrm{T}}^{(0\nu)} \right], \tag{25}$$

where $g_{\mathrm{A}} = 1.25$ corresponds to the bare-nucleon value of the axial-vector coupling constant and $g_{\mathrm{V}} = 1.00$ is the vector coupling constant. The tensor matrix element is neglected in the present calculations since its contribution is very small [28,32].

The Gamow-Teller and Fermi NMEs appearing in the half-life expressions can be written explicitly in the form

$$M_K^{(0\nu)} = \sum_{J^\pi} \sum_{J'} \sum_{k_1 k_2} \sum_{pp'nn'} (-1)^{j_p + j_{n'} + J + J'} \sqrt{2J'+1} \begin{Bmatrix} j_n & j_p & J \\ j_{p'} & j_{n'} & J' \end{Bmatrix} m_K(nn',\, pp';\, J';\, k_1, k_2) \left(0_f^+ \| [c_{n'}^\dagger \tilde{c}_{p'}]_J \| J_{k_1}^\pi\right)$$
$$\times \left\langle J_{k_1}^\pi \middle| J_{k_2}^\pi \right\rangle \left(J_{k_2}^\pi \middle\| [c_n^\dagger \tilde{c}_p]_J \middle\| 0_i^+\right), \quad K = \mathrm{F},\ \mathrm{GT}, \tag{26}$$

where k_1 and k_2 label the different nuclear-model solutions for a given multipole J^π, the set k_1 stemming from the calculation based on the final nucleus and the set k_2 stemming from the calculation based on the initial nucleus. Here the one-body transition densities are $(0_f^+ \| [c_{n'}^\dagger \tilde{c}_{p'}]_J \| J_{k_1}^\pi)$ and $(J_{k_2}^\pi \| [c_n^\dagger \tilde{c}_p]_J \| 0_i^+)$, and they are given separately for the different types of 0^+ final states f in Sec. II C.

The two-particle matrix element of (26) can be written as

$$m_K(nn',\, pp';\, J';\, k_1, k_2) = \widehat{J'} \widehat{j_p} \widehat{j_{p'}} \widehat{j_n} \widehat{j_{n'}} \sum_{\lambda S} (2\lambda+1)(2S+1) F_K \begin{Bmatrix} l_p & l_{p'} & \lambda \\ \frac{1}{2} & \frac{1}{2} & S \\ j_p & j_{p'} & J' \end{Bmatrix} \begin{Bmatrix} l_n & l_{n'} & \lambda \\ \frac{1}{2} & \frac{1}{2} & S \\ j_n & j_{n'} & J' \end{Bmatrix} \sum_{n_1 n_2 l N L} M_\lambda(n_1 l N L; n_n l_n n_{n'} l_{n'})$$
$$\times M_\lambda(n_2 l N L; n_p l_p n_{p'} l_{p'}) \int d^3 r \phi_{n_1 l}(\mathbf{r}) h_K\left(r_{12}, \frac{1}{2}\left[E_{k_1} + E_{k_2}\right]\right) \phi_{n_2 l}(\mathbf{r}), \tag{27}$$

where $\widehat{j} = \sqrt{2j+1}$ and $r_{12} = |\mathbf{r}_1 - \mathbf{r}_2|$ is the relative distance between the two decaying protons. The following auxiliary quantities have been defined:

$$F_{\mathrm{F}} = 1, \quad F_{\mathrm{GT}} = 6(-1)^{S+1} \begin{Bmatrix} \frac{1}{2} & \frac{1}{2} & S \\ \frac{1}{2} & \frac{1}{2} & 1 \end{Bmatrix}. \tag{28}$$

The quantities M_λ are the Moshinsky brackets that mediate the transformation from the laboratory coordinates $\mathbf{r}_1$ and $\mathbf{r}_2$ to the center-of-mass coordinate $\mathbf{R} = \frac{1}{\sqrt{2}}(\mathbf{r}_1 + \mathbf{r}_2)$ and the relative coordinate $\mathbf{r} = \frac{1}{\sqrt{2}}(\mathbf{r}_1 - \mathbf{r}_2)$. In this way the short-range correlations of the two decaying protons are easily incorporated in the theory. The wave functions $\phi_{nl}(\mathbf{r})$ are taken to be the eigenfunctions of the isotropic harmonic oscillator.

The neutrino potential $h_K(r_{12}, E)$, $K = \mathrm{F}, \mathrm{GT}$, in the integral of (27) is defined as

$$h_K(r_{12}, E) = \frac{2}{\pi} R_{\mathrm{A}} \int dq \frac{q h_K(q^2)}{q + E - (E_i + E_f)/2} j_0(q r_{12}), \tag{29}$$

where j_0 is the spherical Bessel function and the integration is performed over the exchanged momentum q. Here $E_i = M_i c^2$ is the ground-state mass energy of the initial nucleus and E_f is the (ground-state or excited-state) mass energy of the final nucleus. In practice the lowest pnQRPA energies of the two sets k_1 and k_2 are normalized such that the energy difference of these energies and the mass energy of the initial nucleus matches the corresponding experimental energy difference. The term $h_K(q^2)$ in Eq. (29) includes the contributions arising

from the short-range correlations, nucleon form factors, and higher-order terms of the nucleonic weak current [28,29].

C. Transition densities

The various transition densities are addressed in this section. The initial-branch transition density remains always the same, namely,

$$\left(J^{\pi}_{k_2}\|[c^{\dagger}_{n}\tilde{c}_{p}]_{J}\|0^{+}_{i}\right) = \widehat{J}(-1)^{j_p+j_n+J+1}\left[v_p u_n X^{J^{\pi}_{k_2}}_{pn} + u_p v_n Y^{J^{\pi}_{k_2}}_{pn}\right]. \tag{30}$$

The transition density corresponding to the final ground state reads

$$\left(0^{+}_{\rm gs}\|[c^{\dagger}_{n'}\tilde{c}_{p'}]_{J}\|J^{\pi}_{k_1}\right) = \widehat{J}(-1)^{j_{p'}+j_{n'}+J+1}\left[\bar{u}_{p'}\bar{v}_{n'}\bar{X}^{J^{\pi}_{k_1}}_{p'n'} + \bar{v}_{p'}\bar{u}_{n'}\bar{Y}^{J^{\pi}_{k_1}}_{p'n'}\right], \tag{31}$$

where v ($\bar{v}$) and u ($\bar{u}$) correspond to the BCS occupation and unoccupation amplitudes of the initial (final) even-even nucleus. The amplitudes X and Y ($\bar{X}$ and $\bar{Y}$) come from the pnQRPA calculation starting from the initial (final) nucleus of the $0\nu2\beta$ decay.

For the excited states the MCM [41,42] is used. It is designed to connect excited states of an even-even reference nucleus to states of the neighboring odd-odd nucleus. The states of the odd-odd nucleus are given by the pnQRPA and the excited states of the even-even nucleus are generated by the (charge-conserving) quasiparticle random-phase approximation described in detail in Ref. [40]. Here, in contrast to Ref. [40], the symmetrized form of the phonon amplitudes is adopted so that the kth J^{π} state can be written as a QRPA phonon in the form

$$\left|I^{\pi}_{k}\ M\right\rangle = Q^{\dagger}\left(I^{\pi}_{k}, M\right)|\mathrm{QRPA}\rangle = \sum_{ab}\left(Z^{I^{\pi}_{k}}_{ab}[a^{\dagger}_{a}a^{\dagger}_{b}]_{IM} - W^{I^{\pi}_{k}}_{ab}[a^{\dagger}_{a}a^{\dagger}_{b}]^{\dagger}_{IM}\right)|\mathrm{QRPA}\rangle. \tag{32}$$

The symmetrized amplitudes Z and W are obtained from the usual ccQRPA amplitudes X and Y [40] through the following transformation:

$$Z^{I^{\pi}_{k}}_{ab} = \begin{cases} X^{I^{\pi}_{k}}_{ab} & \text{if} \quad a = b, \\ \frac{1}{2}X^{I^{\pi}_{k}}_{ab} & \text{if} \quad a < b, \\ \frac{1}{2}X^{I^{\pi}_{k}}_{ba} & \text{if} \quad a > b, \end{cases} \tag{33}$$

and similarly for W in terms of Y.

The ccQRPA phonon defines a state in the final nucleus of the double-β decay. In particular, if this final state is the kth I^{+} state the related transition density, to be inserted in Eqs. (10) and (26), becomes

$$\left(I^{+}_{k}\|[c^{\dagger}_{n'}\tilde{c}_{p'}]_{L}\|J^{\pi}_{k_1}\right) = 2\widehat{I}\widehat{L}\widehat{J}(-1)^{L+I+J}\left(\sum_{p_1}\left[\bar{v}_{p'}\bar{v}_{n'}\bar{X}^{J^{\pi}_{k_1}}_{p_1n'}\bar{Z}^{I^{+}_{k}}_{p'p_1} - \bar{u}_{p'}\bar{u}_{n'}\bar{Y}^{J^{\pi}_{k_1}}_{p_1n'}\bar{W}^{I^{+}_{k}}_{p'p_1}\right]\begin{Bmatrix} J & I & L \\ j_{p'} & j_{n'} & j_{p_1}\end{Bmatrix}\right.$$
$$\left. + \sum_{n_1}(-1)^{I+j_{n'}+j_{n_1}}\left[\bar{u}_{p'}\bar{u}_{n'}\bar{X}^{J^{\pi}_{k_1}}_{p'n_1}\bar{Z}^{I^{+}_{k}}_{n'n_1} - \bar{v}_{p'}\bar{v}_{n'}\bar{Y}^{J^{\pi}_{k_1}}_{p'n_1}\bar{W}^{I^{+}_{k}}_{n'n_1}\right]\begin{Bmatrix} J & I & L \\ j_{n'} & j_{p'} & j_{n_1}\end{Bmatrix}\right) \tag{34}$$

instead of the expression (31) for the ground-state transition. Again v ($\bar{v}$) and u ($\bar{u}$) correspond to the BCS occupation and unoccupation amplitudes of the initial (final) even-even nucleus. The amplitudes X and Y ($\bar{X}$ and $\bar{Y}$) come from the pnQRPA calculation starting from the initial (final) nucleus of the $\beta\beta$ decay. The amplitudes $\bar{Z}$ and $\bar{W}$ are the amplitudes of the kth I^{+} state in the final nucleus.

One can take a $I^{\pi}_{k} = 2^{+}_{1}$ phonon of (32) and build an ideal two-phonon I^{+} state of the form

$$|I^{+}_{\text{2-ph}}\rangle = \frac{1}{\sqrt{2}}[Q^{\dagger}(2^{+}_{1})Q^{\dagger}(2^{+}_{1})]_{I}|\mathrm{QRPA}\rangle. \tag{35}$$

An ideal two-phonon state consists of partner states $I^{\pi} = 0^{+}$, 2^{+}, 4^{+} that are degenerate in energy and are exactly at twice the excitation energy of the 2^{+}_{1} state. In practice this degeneracy is always lifted by the residual interaction between the one- and two-phonon states [44]. The related transition density of the MCM, which can be inserted in Eqs. (10) and (26), attains the form

$$\left(I^{+}_{\text{2-ph}}\|[c^{\dagger}_{n'}\tilde{c}_{p'}]_{L}\|J^{\pi}_{k_1}\right) = \frac{40}{\sqrt{2}}\widehat{I}\widehat{L}\widehat{J}(-1)^{I+J+j_{p'}+j_{n'}}\sum_{p_1n_1}\left[\bar{v}_{p'}\bar{u}_{n'}\bar{X}^{J^{\pi}_{k_1}}_{p_1n_1}\bar{Z}^{2^{+}_{1}}_{p'p_1}\bar{Z}^{2^{+}_{1}}_{n'n_1}\right.$$
$$\left. + \bar{u}_{p'}\bar{v}_{n'}\bar{Y}^{J^{\pi}_{k_1}}_{p_1n_1}\bar{W}^{2^{+}_{1}}_{p'p_1}\bar{W}^{2^{+}_{1}}_{n'n_1}\right]\begin{Bmatrix} j_{p'} & j_{p_1} & 2 \\ j_{n'} & j_{n_1} & 2 \\ L & J & I\end{Bmatrix}, \tag{36}$$

where, as usual, the barred quantities denote amplitudes obtained for the $\beta\beta$ daughter nucleus.

III. MODEL PARAMETERS

The calculations were done in a single-particle space consisting of the $1p$-$0f$-$2s$-$1d$-$0g$-$0h$ shells for both protons and neutrons. The single-particle energies were generated by the use of a spherical Coulomb-corrected Woods–Saxon (WS) potential with a standard parametrization [45], optimized for

nuclei near the line of β stability. The WS bases reproduce satisfactorily the low-energy spectra of the neighboring odd-A nuclei. The Bonn-A G matrix has been used as the two-body interaction and is has been renormalized in the standard way [41,46]. The quasiparticles are treated in the BCS formalism and the pairing matrix elements are scaled by a common factor, separately for protons and neutrons. In practice these factors are fitted such that the lowest quasiparticle energies obtained from the BCS formalism match the experimental pairing gaps for protons and neutrons, respectively.

As explained in detail in Ref. [37] the particle-hole and particle-particle parts of the proton-neutron two-body interaction are separately scaled by the particle-hole parameter $g_{\rm ph}$ and particle-particle parameter $g_{\rm pp}$. The value of the particle-hole parameter, $g_{\rm ph} = 1.50$, was fixed by the available systematics [40] on the location of the Gamow-Teller giant resonance (GTGR) state. The value of the $g_{\rm pp}$ parameter regulates the β^--decay amplitude of the first 1^+ state in the intermediate nucleus [47] and hence also the decay rates of the $\beta\beta$ decays. This value can be fixed by either the data on β^- decays [47] or by the data on $2\nu\beta^-\beta^-$-decay rates within the interval $g_{\rm A} = 1.00$–1.25 of the axial-vector coupling constant [27–29,31]. The experimental error and the uncertainty in the value of $g_{\rm A}$ then induce an interval of physically acceptable values of $g_{\rm pp}$, the minimum value of $g_{\rm pp} = 0.80$ being related to $g_{\rm A} = 1.00$ and the maximum value $g_{\rm pp} = 1.15$ being related to $g_{\rm A} = 1.25$. This particular assignment of a certain $g_{\rm pp}$ to a certain $g_{\rm A}$ is natural because the magnitude of the calculated $2\nu\beta\beta$ NME, $M^{(2\nu)}$, decreases with increasing value of $g_{\rm pp}$ in a pnQRPA calculation [46,48,49] and this magnitude is compared with the magnitude of the experimental NME, $M^{(2\nu)}(\text{exp}) \propto (g_{\rm A})^{-2}$, deduced from the experimental $2\nu\beta\beta$ half-life. The lower limit of $g_{\rm pp}$ is a reasonable choice used, e.g., in the analysis of [21,33]. The upper limit gives the minimum magnitude of the $2\nu\beta\beta$ NME for the ground-state-to-ground-state transition. In this case, thus, the value of the $2\nu\beta\beta$ NME does not degrease monotonically up to the collapse point of the pnQRPA but only up to $g_{\rm pp} = 1.15$, after which it starts to rise again. This same behavior of the $2\nu\beta\beta$ NME was registered in the studies of Refs. [10,21]. The wide range of the chosen values of $g_{\rm pp}$, $g_{\rm pp} = 0.80$–1.15 guarantees that all the physically meaningful values of the $2\nu2\beta$ and $0\nu2\beta$ NMEs are covered.

For the ccQRPA the $g_{\rm ph}$ and $g_{\rm pp}$ parameters were fixed to the values $g_{\rm ph} = 0.739$ and $g_{\rm pp} = 1.00$ for the 2^+ channel. For the given value of $g_{\rm ph}$ the experimental location of the 2^+_1 state in ^{96}Mo is reproduced by the calculations. For the 0^+ channel the values $g_{\rm ph} = 0.378$ and $g_{\rm pp} = 0.975$ push the energy of the lowest ccQRPA root (which is a spurious state [50]) to zero and make the second root roughly reproduce the experimental excitation energy of the 0^+_1 state.

IV. TWO-NEUTRINO DOUBLE-β DECAYS

In Table I are shown the values of the $2\nu2\beta$ half-lives for different modes of decay, as deduced from Eqs. (6)–(8). The first column gives the final state and the second column its interpretation as the QRPA ground state (gs) or a one-phonon state (1-ph) [see (32)] or a two-phonon state (2-ph) [see (35)]. The computed half-life ranges for the different $2\nu2\beta$ decay modes have been quoted in the last three columns.

The rather wide ranges of half-lives quoted in the table stem from two sources of uncertainty. One source of uncertainty is the range $g_{\rm pp} = 0.80$–1.15 of the values of the particle-particle strength parameter discussed in Sec. III. The other source of uncertainty is the unknown experimental excitation energy of the first 1^+ state in the intermediate nucleus ^{96}Tc. This is needed in defining the exact value of Δ_k in Eq. (5). In the present calculations a wide range of excitation energies, $E_{\rm exc}(1^+_1) = 0.0$–2.0 MeV, was chosen. The lower (upper) limit of this range corresponds to the lower (upper) limit of the half-life in Table I since then the value of Δ_k is the minimum (maximum) and thus the NME attains its maximum (minimum) value.

The value of the axial-vector coupling constant $g_{\rm A}$ strongly affects the magnitudes of the phase-space factors $G^{\alpha}_{2\nu}(I^+)$ in Eqs. (6)–(8). This dependence of the phase-space factors is stronger than the dependence of the NME on $g_{\rm pp}$ and is in the opposite direction. This means that the lower (upper) limits of the half-lives in Table I correspond to $g_{\rm A} = 1.25$ ($g_{\rm A} = 1.00$). The only exception to this pattern is the behavior of the transition to the final 2^+_1 state, where the opposite is true, and hence the words "upper" and "lower" of the previous sentence should be exchanged.

It is well visible in Table I that the half-lives corresponding to the 2^+ final states are much longer than the ones

TABLE I. Values of half-lives for the various $2\nu2\beta$ processes in ^{96}Ru. The first column gives the final state, the second the interpretation in terms of one-phonon (1-ph) and two-phonon (2-ph) ccQRPA structures, and the last three columns the half-lives in units of years for different modes of the decay.

Final state	Structure	Mode		
		ECEC (yr)	β^+EC (yr)	$\beta^+\beta^+$ (yr)
$0^+_{\rm gs}$	gs	$(4.7$–$39) \times 10^{20}$	$(2.0$–$23) \times 10^{21}$	$(1.2$–$10) \times 10^{26}$
2^+_1	1-ph	4.2×10^{28}–2.2×10^{32}	1.3×10^{27}–1.2×10^{31}	Q forbidden
0^+_1	1-ph	$(4.2$–$92) \times 10^{21}$	$(6.1$–$190) \times 10^{24}$	Q forbidden
0^+_2	2-ph	$(3.6$–$54) \times 10^{23}$	$(7.5$–$150) \times 10^{27}$	Q forbidden
2^+_2	2-ph	$(1.8$–$6500) \times 10^{29}$	2.1×10^{33}–1.6×10^{37}	Q forbidden
2^+_3	1-ph	$>1.6 \times 10^{29}$	$>3.4 \times 10^{38}$	Q forbidden

TABLE II. Absolute values of NMEs for the various $2\nu2\beta$ processes in ^{96}Ru. The first column gives the final state and the next columns the absolute values of the NMEs $M^{\alpha}_{2\nu}$ of (9).

Final state	$\lvert M^{\alpha}_{2\nu}\rvert$				
	$\beta^+\beta^+$	β^+EC(K)	β^+EC(L)	EC(K)EC(K)	EC(K)EC(L)
0^+_{gs}	0.2075–0.7185	0.4321–1.6885	0.4329–1.7017	0.4150–1.4370	0.4150–1.4371
2^+_1	0.0001–0.0064	0.0001–0.0117	0.0001–0.0120	0.0001–0.0084	0.0001–0.0084
0^+_1	0.2460–0.7771	0.5024–1.8564	0.5031–1.8802	0.4920–1.5542	0.4920–1.5544
0^+_2	0.0406–0.1410	0.0824–0.3363	0.0824–0.3410	0.0812–0.2820	0.0812–0.2821
2^+_2	0.0002–0.0101	0.0003–0.0273	0.0003–0.0282	0.0003–0.0188	0.0003–0.0188
2^+_3	<0.0107	<0.0318	<0.0329	<0.0216	<0.0216

corresponding to the 0^+ final states. This stems from the fact that the related NMEs are much smaller for the 2^+ final states. This feature was discussed already in the early work of [12]. The magnitudes of such small NMEs are very sensitive to the adopted value of excitation energy of the first 1^+ state in the intermediate nucleus. That is why the ranges of half-lives are much wider for the decays to the 2^+ final states than for the decays to the 0^+ final states. The situation is clarified by Table II, where the ranges of absolute values of the NMEs involved in Eqs. (6)–(8) have been summarized. It is interesting to note that the NME for the 2^+_3 final state crosses zero in the investigated interval and thus the lower limit zero is reached for the absolute value of the NME (see the last line of Table II).

Concerning the detection possibilities of the $2\nu2\beta$ processes in ^{96}Ru, the best chances of detection in the near future are offered by the ECEC and β^+EC decays to the ground state with the computed half-lives in the range of $(5–230) \times 10^{20}$ yr. Also the ECEC decay to the first excited 0^+ state at 1148.13 keV of excitation is within reach of future experiments with the computed half-lives in the range of $(4.2–92) \times 10^{21}$ yr. The best experimental limits thus far have been set by using the ultra-low background HPGe γ spectrometry in Ref. [51]. Sensitivities in the range of 10^{18}–10^{19} yr have been achieved. At present these experiments are expected to come close to the sensitivity limit of 10^{20} yr. It seems that in general the detection of the decays to the 2^+ final states is hopeless in the near future.

V. NEUTRINOLESS DOUBLE-β DECAYS

We now turn to the calculations of the observables related to $0\nu2\beta$ decays. As discussed in Sec. III the increasing value of g_A can be related to the increasing value of g_{pp}. In the present calculations the value $g_{pp} = 0.80$ is associated with $g_A = 1.00$ and the value $g_{pp} = 1.15$ is associated with $g_A = 1.25$. The value $g_{pp} = 1.15$ was chosen because it produces the minimum value of the $2\nu2\beta$ NME for the ground-state transition. This value is not very far from the collapse point of the pnQRPA but is chosen to have a wide range of g_{pp} values to see how the magnitudes of the $0\nu2\beta$ NMEs vary in this range. The smaller value $g_{pp} = 0.80$ was chosen such that the available range of g_{pp} values would be wide enough to confine the possible values of the $0\nu2\beta$ NMEs. The Jastrow- and UCOM-correlated NMEs calculated in this way are shown in Table III.

In Table III the first column lists the NMEs for different final states in ^{96}Mo, namely, the ground state, the first excited 0^+ state, 0^+_1 at 1148.13 keV of excitation, the second excited 0^+ state, presumed to be a two-phonon state, $0^+_{2\text{-ph}}$, at 1330 keV of excitation, and the resonant state at 2712.68 keV of excitation. Here we assume the spin-parity 0^+ for the resonant state, denoted by 0^+_{res}. The values of the Gamow-Teller, Fermi, and total NMEs have been given for both Jastrow and UCOM short-range correlations and the two extreme values of the axial-vector coupling constant.

From Table III one observes interesting details: typically the UCOM-correlated NMEs are larger than the Jastrow-correlated ones due to the less sharp cut of the relative two-nucleon wave function at short distances [27,31]. This same pattern can be observed in the present calculations for the ground-state NME and the NMEs corresponding to the one-phonon states 0^+_1 and 0^+_{res}. This occurs because the

TABLE III. The computed Jastrow and UCOM correlated NMEs for the ground-state and excited-state decays of ^{96}Ru. The 0^+_2 state is described as a coupling of two 2^+_1 ccQRPA phonons and the 0^+_1 and 0^+_{res} states are described by one ccQRPA phonon.

NME	Jastrow		UCOM	
	$g_A = 1.00$	$g_A = 1.25$	$g_A = 1.00$	$g_A = 1.25$
$M^{(0\nu)}_{GT}(0^+_{gs})$	4.272	2.589	5.279	3.467
$M^{(0\nu)}_{F}(0^+_{gs})$	−1.560	−0.988	−1.877	−1.279
$M^{(0\nu)'}(0^+_{gs})$	3.733	3.222	4.580	4.285
$M^{(0\nu)}_{GT}(0^+_1)$	1.046	2.004	1.087	2.045
$M^{(0\nu)}_{F}(0^+_1)$	−0.237	−0.396	−0.249	−0.409
$M^{(0\nu)'}(0^+_1)$	0.821	2.258	0.855	2.307
$M^{(0\nu)}_{GT}(0^+_{2\text{-ph}})$	0.353	0.394	0.329	0.371
$M^{(0\nu)}_{F}(0^+_{2\text{-ph}})$	−0.211	−0.204	−0.212	−0.205
$M^{(0\nu)'}(0^+_{2\text{-ph}})$	0.360	0.524	0.346	0.502
$M^{(0\nu)}_{GT}(0^+_{res})$	3.259	4.846	3.507	5.097
$M^{(0\nu)}_{F}(0^+_{res})$	−0.526	−0.650	−0.610	−0.734
$M^{(0\nu)'}(0^+_{res})$	2.423	5.262	2.635	5.567

decomposition of these NMEs in terms of multipoles looks qualitatively similar (see below). Quite the contrary is true for the two-phonon (0_1^+) state: the UCOM NME is smaller than the Jastrow NME. This strange behavior is explained by the very different qualitative behavior of the multipole decomposition—as shown below, the J' decomposition [see Eq. (37)] in this case consists of contributions of wildly alternating signs.

It is interesting to note that the one-phonon NMEs have quite big magnitudes, of the same order as the ground-state NME. The same feature of the 0_1^+ state was observed in Ref. [52] for the $0\nu2\beta^-$ decay of ^{96}Zr, thus making it an interesting state with respect to experimental observation of double-β decay to an excited state.

As already indicated above, the $0\nu\beta\beta$ NMEs $M^{(0\nu)'}$ can be decomposed into contributions of different intermediate multipoles. This decomposition can be made in two ways, either through the different multipole states J^π of the intermediate nucleus (in this case the states of ^{96}Tc) or through different couplings J' of the two decaying nucleons [31,53]. For the Gamow-Teller NME these decompositions can be schematically written as

$$M_{\rm GT}^{(0\nu)} = \sum_{J^\pi} \sum_{J'} M_{\rm GT}^{(0\nu)}(J^\pi, J'), \tag{37}$$

where $M_{\rm GT}^{(0\nu)}(J^\pi, J')$ is given explicitly in Eq. (26). The decompositions (37) are shown for the Gamow-Teller NMEs of the decays of ^{96}Ru in Figs. 2–5. All the figures refer to calculations using the Jastrow short-range correlations and the value $g_{\rm A} = 1.25$ for the axial-vector coupling constant.

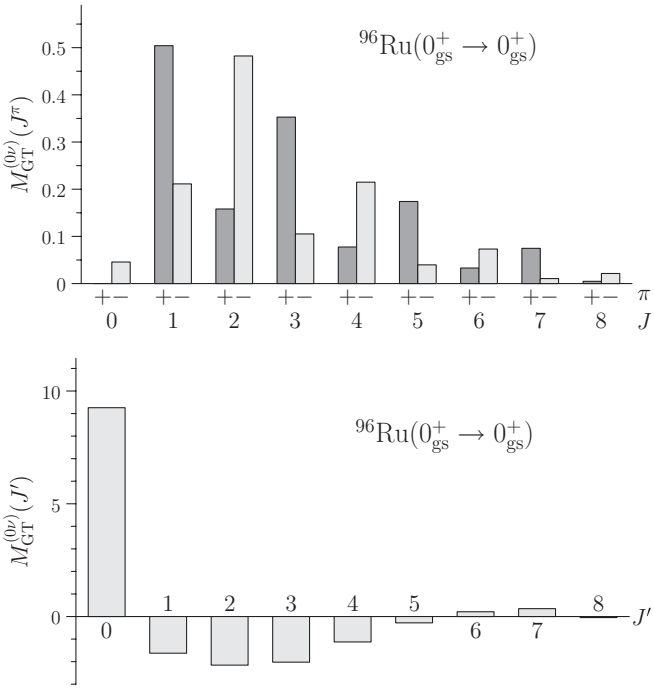

FIG. 2. Decompositions of (37) in J^π (upper panel) and J' (lower panel) for the ground-state Gamow-Teller $M_{\rm GT}^{(0\nu)}(0_{\rm gs}^+)$ NME of ^{96}Ru. Results for the Jastrow short-range correlations are shown with $g_{\rm A} = 1.25$.

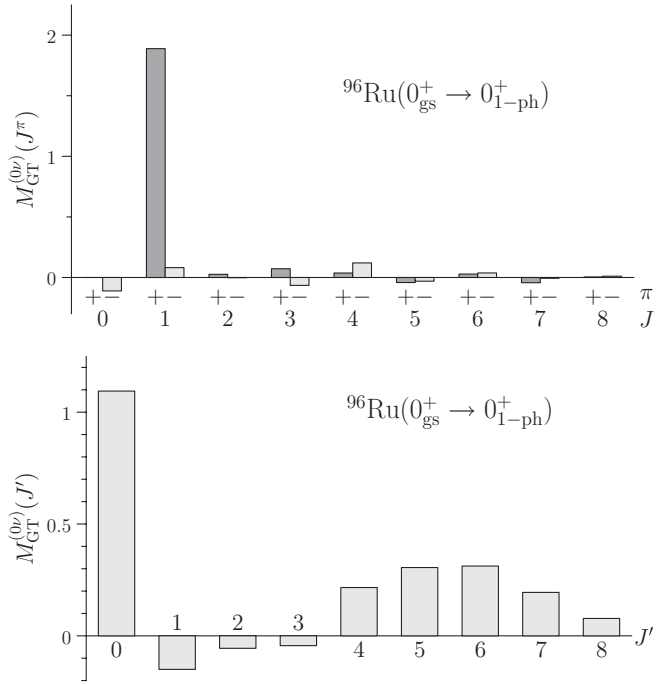

FIG. 3. The same as in Fig. 2 for the one-phonon NME $M_{\rm GT}^{(0\nu)}(0_{\rm 1\text{-}ph}^+)$ corresponding to the 0_1^+ state at 1148.13 keV in ^{96}Mo.

From the decomposition figures one can make the following general observations: For the ground-state NME the decomposition in terms of J^π is the typical one of the pnQRPA calculations [31,37] and the decomposition in terms of J' is typical of the shell-model [53] and pnQRPA [21,31] calculations. Here typical for the J^π decomposition are the strong contributions of the high-multipole components 2^-, 3^+, 4^-, and 5^+ and the relatively strong 1^+ contribution (which depends strongly on the value of the strength parameter $g_{\rm pp}$). For the J' decomposition typical is the large positive monopole contribution and the much smaller, mostly negative, higher-multipole contributions.

For the lowest one-phonon 0^+ state, $0_1^+ = 0_{\rm 1\text{-}ph}^+$, the pattern is qualitatively different for the J^π decomposition since the multipole components other than 1^+ are strongly suppressed. In the case of the J' decomposition the majority of the higher-multipole contributions are positive instead of negative. The multipole decompositions of the 0^+ resonant state, $0_{\rm res}^+$, which is also a one-phonon ccQRPA state, follow pretty much the same pattern. The behavior of the two-phonon ($0_{\rm 2\text{-}ph}^+$) NME is qualitatively totally different: The J' decomposition has both large positive and large negative contributions and the monopole component is no longer the dominant one. The alternating structure of this decomposition conspires to produce larger Jastrow than UCOM NMEs. For the J^π decomposition the 1^+ contribution is the predominant one.

The NMEs of Table III can be combined with the appropriate phase-space factors to produce predicted half-lives for a given value of the effective neutrino mass $\langle m_\nu \rangle$. The half-lives of the different $0\nu2\beta$ modes can be compactly

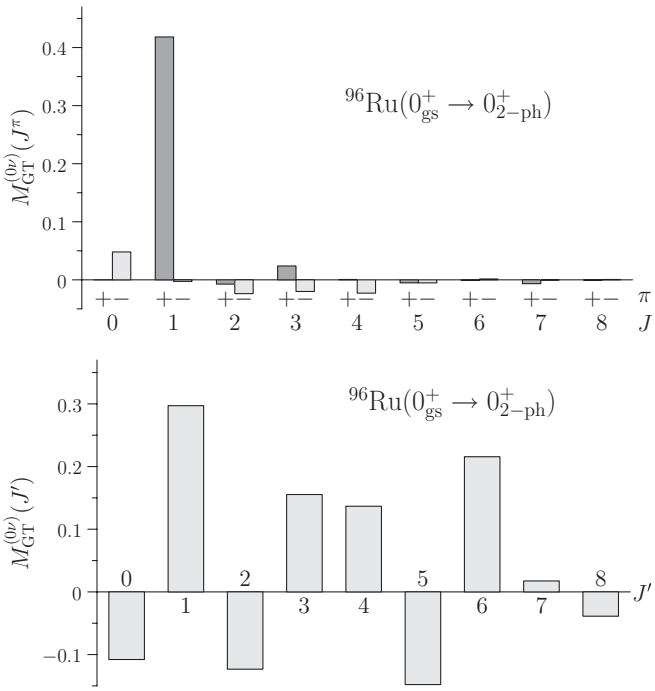

FIG. 4. The same as in Fig. 2 for the two-phonon NME $M^{(0\nu)}_{GT}(0^+_{2\text{-ph}})$ corresponding to the 0^+_2 state at 1330 keV in ^{96}Mo.

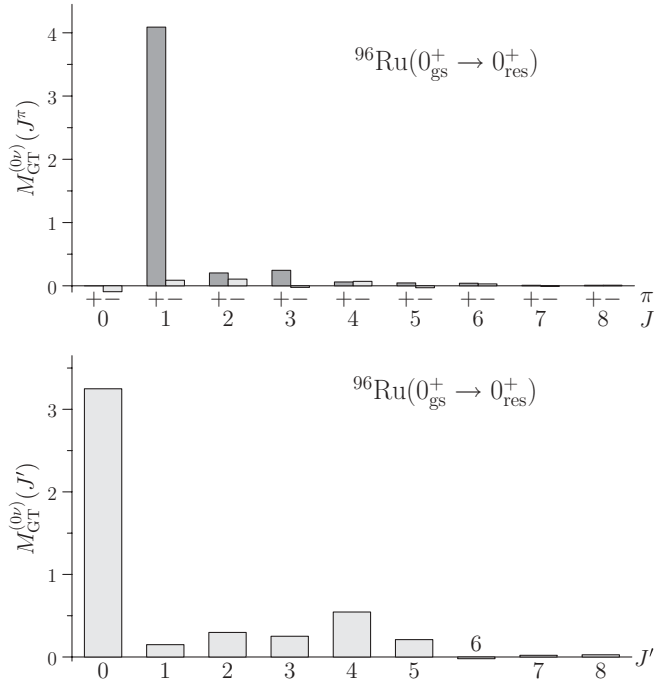

FIG. 5. The same as in Fig. 2 for the resonance NME $M^{(0\nu)}_{GT}(0^+_{res})$ corresponding to the 0^+ state at 2712.68 keV in ^{96}Mo.

written as

$$T^{\beta^+\beta^+}_{1/2} = T^{\beta^+\beta^+}_0(\langle m_\nu\rangle\ [\text{eV}])^{-2}, \tag{38}$$

$$T^{\beta^+\text{EC}}_{1/2} = T^{\beta^+\text{EC}}_0(\langle m_\nu\rangle\ [\text{eV}])^{-2}, \tag{39}$$

$$T^{\text{ECEC}}_{1/2} = T^{\text{ECEC}}_0(\langle m_\nu\rangle\ [\text{eV}])^{-2}, \tag{40}$$

where the effective neutrino mass should be inserted in units of electron volts. In Table IV the auxiliary factors of the above equations are given for both the Jastrow and UCOM short-range correlations.

From Table IV one observes that for the decay to the ground state the range of half-lives is rather narrow in spite of the wide range of values of g_{pp} used in the calculations. In contrast to this, for the other decays the range of half-lives is wide. The g_{pp} dependence of the corresponding transition amplitudes arises mainly from the g_{pp} dependence of the 1^+ multipole. In the present case Table III tells us that in fact the Gamow-Teller and Fermi NMEs change quite a bit for the ground-state transition but this change is compensated by the change in the value of g_A in the definition of the total NME $M^{(0\nu)'}$. For the excited-state transitions the changes in the individual NMEs are in directions that are generally opposite to the ones of the ground-state NME and this conspires to produce large variations for the total NME. The absolute variation of the two-phonon NME with varying g_A is, in fact, quite small when compared to the variation of the NMEs corresponding to the other decay transitions. The weak dependence on g_{pp} of the two-phonon NMEs is well known from the earlier works [12,54] for $0\nu2\beta^-$ decays.

Table IV indicates that the best detection possibilities are for the β^+EC decay to the ground state with the half-lives being in the range of (6–10) $\times 10^{28}$ yr for an effective neutrino mass of 0.1 eV. For the $\beta^+\beta^+$ mode the half-lives are one order of magnitude longer. Decays to the excited states will be very hard to detect. Also the resonant 0νECEC decay is extremely hard to detect, with the predicted half-lives exceeding 10^{33} yr for effective neutrino masses of tenths of an electron volt. The reason for this long half-life of this decay mode is the badly fulfilled resonance condition in the half-life expression (22). In this case the degeneracy parameter has the value $|Q - E| =$ 3.90 keV and thus is, unfortunately, in the keV range instead of the desired eV range of energies. One should also point out that the 0^+ assignment for the spin-parity of the resonant state is unlikely [23] and the angular momentum of the state is likely to be higher. This would lead to an increase of the estimated half-life and would render the R0νECEC transition even harder to detect.

TABLE IV. The auxiliary factors of Eqs. (38)–(40) for the decays of ^{96}Ru.

State	s.r.c.	T_0		
		$\beta^+\beta^+$ (10^{27} yr)	β^+EC (10^{26} yr)	R0νECEC (10^{31} yr)
0^+_{gs}	UCOM	5.89–6.72	4.97–5.68	
	Jastrow	8.86–11.9	7.48–10.0	
0^+_1	UCOM		104–756	
	Jastrow		108–819	
$0^+_{2\text{-ph}}$	UCOM		3400–7300	
	Jastrow		3200–6700	
0^+_{res}	UCOM			4.37–19.5
	Jastrow			4.89–23.0

VI. SUMMARY AND CONCLUSIONS

The various modes of two-neutrino and neutrinoless double-β decays of ^{96}Ru have been investigated for the associated nuclear matrix elements and decay half-lives. A QRPA-based theory framework with G-matrix-based two-body interactions and realistically large single-particle bases has been used in the calculations. The computed values of the nuclear matrix elements have been tabulated by taking into account their theoretical error limits. The half-lives corresponding to these matrix elements have been tabulated for two different short-range correlations.

The two-neutrino ECEC and β^+EC double-β decays to the ground state and the ECEC decay to the first excited 0^+ state at 1148.13 keV of excitation have computed half-lives in the range of (5–920) $\times$ 10^{20} yr and thus are potentially detectable in (near) future experiments. The range of half-lives for the neutrinoless double-β decays starts from 10^{28} yr for effective neutrino masses of a few tenths of an electron volt.

The computed half-life for the experimentally interesting resonant neutrinoless double electron capture turns out to be more than 10^{33} yr for a neutrino mass of 0.1 eV. Hence, this decay mode seems to be extremely hard to measure in future experiments.

ACKNOWLEDGMENT

This work was supported by the Academy of Finland under the Finnish Center of Excellence Program 2012-2017 (Nuclear and Accelerator Based Program at JYFL).

[1] M. Doi, T. Kotani, and E. Takasugi, Prog. Theor. Phys. Suppl. **83**, 1 (1985).
[2] J. Suhonen and O. Civitarese, Phys. Rep. **300**, 123 (1998).
[3] F. T. Avignone III, S. R. Elliott, and J. Engel, Rev. Mod. Phys. **80**, 481 (2008).
[4] A. S. Barabash, Phys. Rev. C **81**, 035501 (2010).
[5] M. Doi and T. Kotani, Prog. Theor. Phys. **87**, 1207 (1992).
[6] M. Doi and T. Kotani, Prog. Theor. Phys. **89**, 139 (1993).
[7] J. Bernabeu, A. De Rujula, and C. Jarlskog, Nucl. Phys. B **223**, 15 (1983).
[8] Z. Sujkowski and S. Wycech, Phys. Rev. C **70**, 052501 (2004).
[9] A. Staudt, K. Muto, and H. V. Klapdor-Kleingrothaus, Phys. Lett. B **268**, 312 (1991).
[10] J. Suhonen, Phys. Rev. C **48**, 574 (1993).
[11] M. Hirsch, K. Muto, T. Oda, and H. Klapdor-Kleingrothaus, Z. Phys. A **347**, 151 (1994).
[12] M. Aunola and J. Suhonen, Nucl. Phys. A **602**, 133 (1996).
[13] J. Suhonen and M. Aunola, Nucl. Phys. A **723**, 271 (2003).
[14] J. Suhonen, S. B. Khadkikar, and A. Faessler, Phys. Lett. B **237**, 8 (1990).
[15] J. Suhonen, S. B. Khadkikar, and A. Faessler, Nucl. Phys. A **529**, 727 (1991).
[16] J. Suhonen, S. B. Khadkikar, and A. Faessler, Nucl. Phys. A **535**, 509 (1991).
[17] M. Doi, T. Kotani, H. Nishiura, and E. Takasugi, Prog. Theor. Phys. **69**, 602 (1983).
[18] S. Rahaman *et al.*, Phys. Lett. B **662**, 111 (2008).
[19] V. Kolhinen, V. Elomaa, T. Eronen, J. Hakala, A. Jokinen, M. Kortelainen, J. Suhonen, and J. Äystö, Phys. Lett. B **684**, 17 (2010).
[20] V. S. Kolhinen, T. Eronen, D. Gorelov, J. Hakala, A. Jokinen, A. Kankainen, J. Rissanen, J. Suhonen, and J. Äystö, Phys. Lett. B **697**, 116 (2011).
[21] J. Suhonen, Phys. Lett. B **701**, 490 (2011).
[22] J. Suhonen, Eur. Phys. J. A **48**, 51 (2012).
[23] M. I. Krivoruchenko, F. Šimkovic, D. Frekers, and A. Faessler, Nucl. Phys. A **859**, 140 (2011).
[24] T. Tomoda, Phys. Lett. B **474**, 245 (2000).
[25] G. A. Miller and J. E. Spencer, Ann. Phys. (NY) **100**, 562 (1976).
[26] H. Feldmeier, T. Neff, R. Roth, and J. Schnack, Nucl. Phys. A **632**, 61 (1998).
[27] M. Kortelainen, O. Civitarese, J. Suhonen, and J. Toivanen, Phys. Lett. B **647**, 128 (2007).
[28] M. Kortelainen and J. Suhonen, Phys. Rev. C **75**, 051303(R) (2007).
[29] M. Kortelainen and J. Suhonen, Phys. Rev. C **76**, 024315 (2007).
[30] J. Suhonen and M. Kortelainen, Int. J. Mod. Phys. E **17**, 1 (2008).
[31] F. Šimkovic, A. Faessler, V. Rodin, P. Vogel, and J. Engel, Phys. Rev. C **77**, 045503 (2008).
[32] J. Menéndez, A. Poves, E. Caurier, and F. Nowacki, Nucl. Phys. A **818**, 139 (2009).
[33] J. Suhonen, Nucl. Phys. A **864**, 63 (2011).
[34] F. Šimkovic, G. Pantis, J. D. Vergados, and A. Faessler, Phys. Rev. C **60**, 055502 (1999).
[35] S. Eliseev *et al.*, Phys. Rev. C **83**, 038501 (2011).
[36] ENSDF at the National Nuclear Data Center site, http://www.nndc.bnl.gov.
[37] J. Suhonen and O. Civitarese, Nucl. Phys. A **847**, 207 (2010).
[38] J. Suhonen, Int. J. Mod. Phys. E **20**, 451 (2011).
[39] J. Suhonen, Nucl. Phys. A **853**, 36 (2011).
[40] J. Suhonen, *From Nucleons to Nucleus: Concepts of Microscopic Nuclear Theory* (Springer, Berlin, 2007).
[41] J. Suhonen, Nucl. Phys. A **563**, 205 (1993).
[42] O. Civitarese and J. Suhonen, Nucl. Phys. A **575**, 251 (1994).
[43] B. Crasemann, *Atomic Inner-Shell Processes* (Academic, New York, 1975).
[44] D. S. Delion and J. Suhonen, Phys. Rev. C **67**, 034301 (2003).
[45] A. Bohr and B. R. Mottelson, *Nuclear Structure,* Vol. I (Benjamin, New York, 1969).
[46] J. Suhonen, T. Taigel, and A. Faessler, Nucl. Phys A **486**, 91 (1988).
[47] J. Suhonen, Phys. Lett. B **607**, 87 (2005).
[48] P. Vogel and M. R. Zirnbauer, Phys. Rev. Lett. **57**, 3148 (1986).
[49] O. Civitarese, A. Faessler, and T. Tomoda, Phys. Lett. B **194**, 11 (1987).
[50] M. Baranger, Phys. Rev. **120**, 957 (1960).
[51] P. Belli *et al.*, Eur. Phys. J. A **42**, 171 (2009).
[52] J. Suhonen, Phys. Rev. C **62**, 042501(R) (2000).
[53] E. Caurier, J. Menéndez, F. Nowacki, and A. Poves, Phys. Rev. Lett. **100**, 052503 (2008).
[54] M. Aunola and J. Suhonen, Nucl. Phys. A **643**, 207 (1998).